Available online at www.sciencedirect.com

ScienceDirect

Nuclear Instruments and Methods in Physics Research A 580 (2007) 427–429

NUCLEAR INSTRUMENTS & METHODS IN PHYSICS RESEARCH Section A

www.elsevier.com/locate/nima

Evaluation of high packing density powder X-ray screens by Monte Carlo methods

P. Liaparinos[a], I. Kandarakis[b], D. Cavouras[b], N. Kalivas[c], H. Delis[a], G. Panayiotakis[a,*]

[a]Department of Medical Physics, Medical School, University of Patras, 26500 Patras, Greece
[b]Department of Medical Instruments Technology, Technological Educational Institution of Athens, Ag. Spyridonos Street, Aigaleo, 12210 Athens, Greece
[c]Greek Atomic Energy Commission, 15310 Athens, Greece

Available online 16 May 2007

Abstract

Phosphor materials are employed in intensifying screens of both digital and conventional X-ray imaging detectors. High packing density powder screens have been developed (e.g. screens in ceramic form) exhibiting high-resolution and light emission properties, and thus contributing to improved image transfer characteristics and higher radiation to light conversion efficiency. For the present study, a custom Monte Carlo simulation program was used in order to examine the performance of ceramic powder screens, under various radiographic conditions. The model was developed using Mie scattering theory for the description of light interactions, based on the physical characteristics (e.g. complex refractive index, light wavelength) of the phosphor material. Monte Carlo simulations were carried out assuming: (a) X-ray photon energy ranging from 18 up to 49 keV, (b) Gd_2O_2S:Tb phosphor material with packing density of 70% and grain size of 7 μm and (c) phosphor thickness ranging between 30 and 70 mg/cm^2. The variation of the Modulation Transfer Function (MTF) and the Luminescence Efficiency (LE) with respect to the X-ray energy and the phosphor thickness was evaluated. Both aforementioned imaging characteristics were shown to take high values at 49 keV X-ray energy and 70 mg/cm^2 phosphor thickness. It was found that high packing density screens may be appropriate for use in medical radiographic systems.

PACS: 02.50.N; 29.40.M

Keywords: X-ray imaging; Phosphor screens; Monte Carlo

1. Introduction

Radiation detectors employed in imaging systems consist of a scintillator coupled to an optical sensor (film, photodiode, photocathode, etc). Scintillator performance is of crucial importance in the design of medical imaging systems. Brightness, spatial resolution and signal-to-noise (S/N) ratio, are imaging characteristics often employed to estimate the quality of a medical image [1,2]. These characteristics are associated to the scintillator's efficiency, which is determined by its radiation absorption and light emission properties [3]. The amount of the emitted light as well as its spatial distribution depend on the type of scintillator (phosphor) material. In ordinary X-ray imaging detectors, this material is embedded within the detector in the form of a granular phosphor screen, i.e., a thin layer consisting of closely packed scintillating grains [4].

Currently screens of ceramic form have been prepared with grain packing density higher than conventional screens (e.g. phosphor packing density of approximately 50%) [5,6]. High packing density affects the light propagation within the phosphor mass as well as the overall optical properties of the scintillator, i.e., increased amount of light scattering.

Spatial resolution and, in some cases light collection, are found improved in high packing density screens [7]. In the present study, the performance of high packing density (e.g. packing density 70%) Gd_2O_2S:Tb phosphor screens was examined by Monte Carlo methods. The Modulation Transfer Function (MTF) as well as the Luminescence Efficiency (LE) were evaluated under X-ray

*Corresponding author. Tel./fax: +30 2610 99613.
E-mail address: panayiot@upatras.gr (G. Panayiotakis).

0168-9002/$ - see front matter
doi:10.1016/j.nima.2007.05.070

mammographic and radiographic conditions (X-ray energy range: 18–49 keV; phosphor thickness: 30–70 mg/cm^2). A self-developed Monte Carlo model [7] based on Mie scattering theory [8–10], was employed in the present work. The Monte Carlo code has been previously validated against published data [7].

2. Materials and methods

The Monte Carlo simulation code [7] was based on: (a) the description of the principal X-ray interactions within the phosphor mass (photoelectric effect, inelastic scattering and elastic scattering) [11–13] (b) the emission of either K-characteristic radiation or Auger electron [14] and (c) the light diffusion assuming local light deposition in the light photon interaction depth. The free path length as well as the probability of light absorption in each light interaction event with a phosphor grain was decided through the Mie scattering algorithm [8–10]. The light scattering angles were sampled according to the Henyey–Greenstein distribution [15]. The model was suitably developed so that only physical (complex refractive index, light wavelength) and structural (grain size, packing density) characteristics of the phosphor are required as input data to estimate the imaging properties of a screen. [7].

When X-ray energy deposition takes place, light photons are intrinsically created following an isotropic distribution. During their propagation within the screen material, light photons interact with the phosphor suffering attenuation by the phosphor grains. At each light interaction site, the interaction type is decided according to the relative probabilities of light absorption and light scattering effects, as follows:

$$m_{\mathrm{abs}} = V_{\mathrm{d}} A Q_{\mathrm{abs}} \quad \text{and} \quad m_{\mathrm{sct}} = V_{\mathrm{d}} A Q_{\mathrm{sct}}, \tag{1}$$

where $m_{\mathrm{abs}}, m_{\mathrm{sct}}$ are the light absorption and light scattering coefficients, respectively. Each coefficient depends on the volume density of the phosphor screen V_{d}, on the geometrical cross-section A of the grain, as well as on the corresponding absorption Q_{abs} and scattering Q_{sct} efficiency factors [8–10].

When light scattering occurs, the azimuthal angle ϕ of the scattered photon is sampled randomly in the interval [0,2π]. The polar angle θ is sampled from the Henyey–Greenstein [15,16] distribution as follows:

$$\cos\,\theta = \frac{1}{2g}\left[1 + g^2 - \left(\frac{1-g^2}{1-g+2gR}\right)^2\right], \tag{2}$$

when $g \neq 0$, where the free parameter g is the anisotropy factor [8,15], which implies isotropic distribution of light for $g = 0$ and sharply forward direction of light for $g = 1$.

Simulations were performed for the widely used and commercially available Gd_2O_2S:Tb phosphor material by taking into account the phosphor grain size and the packing density equal to 7 μm and 70%, respectively. Data were obtained by considering monoenergetic beams with energy ranging from 18 up to 49 keV and for phosphor coating thickness varying from 30 up to 70 mg/cm^2. That was done in order to investigate the performance of the high packing density screens under mammographic (thickness: 30 mg/cm^2; mean X-ray energy: 18 keV) and general radiographic (thickness: 70 mg/cm^2; mean X-ray energy: 49 keV) conditions. Light reflection between screen's surface and the optical detector (e.g. photocathode and film) was not taken into account in the obtained results by the Monte Carlo evaluation.

3. Results and discussion

The LE of high packing density Gd_2O_2S:Tb phosphor material (packing density: 70%), within the X-ray energy range from 18 up to 49 keV, is shown in Table 1. Data are provided for phosphor coating weight ranging from 30 up to 70 mg/cm^2. LE values were obtained by the light emitted from the non-irradiated screen surface (transmission mode).

Above 20 keV, LE was found to increase as phosphor thickness increases. The highest amount of the gained light of specific X-ray energy with respect to phosphor thickness was observed at 49 keV. It was found that at 32 and 49 keV, the light emitted by the 70 mg/cm^2 screen was approximately two times higher than that of the 30 mg/cm^2 screen. This is because, at relatively higher energies, a large portion of incident X-rays is absorbed deeply within the phosphor mass. Light photons, created at the sites of primary X-ray interaction, suffer low attenuation, since they travel short distances to escape the rear side of the screen. On the other hand, below 20 keV, X-ray photon energy is deposited mainly within phosphor layers close to the irradiated surface. Therefore, light photons interact with a large number of grains before they escape the non-irradiated surface of the screen. This increases light attenuation resulting in lower LE values.

The MTF curve of two different values of phosphor thickness, 30 and 70 mg/cm^2, is illustrated in Figs. 1 and 2, respectively. MTF data are provided in the corresponding thickness for X-ray energies 18 and 49 keV for comparison reasons.

Table 1
Variation of luminescence efficiency with respect to phosphor thickness (30–70 mg/cm^2) for X-ray energy ranging from 18 up to 49 keV

Thickness (mg/cm^2)	Luminescence efficiency (arbitrary units)			
	X-ray energy (keV)			
	18	22	32	49
30	0.65	0.64	0.49	0.26
50	0.66	0.81	0.71	0.40
70	0.57	0.82	0.87	0.55

Data concern Gd_2O_2S:Tb phosphor material of packing density 70%.

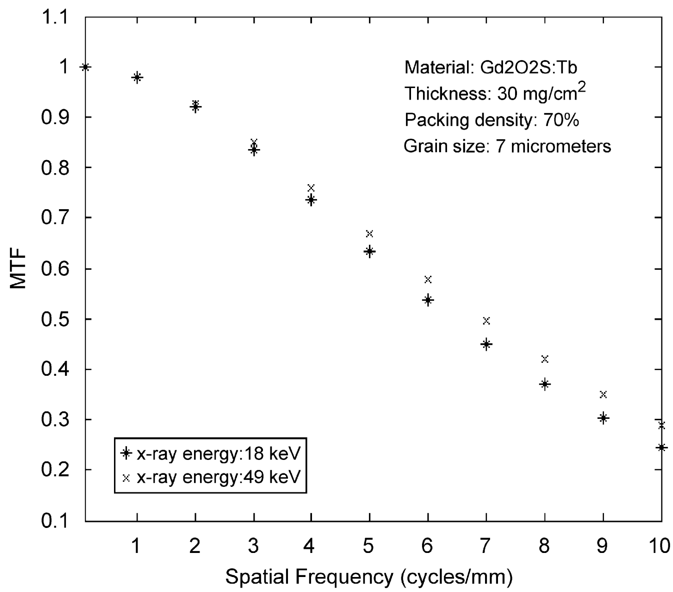

Fig. 1. The variation of MTF as a function of spatial frequency. MTF data are given for phosphor thickness 70 mg/cm^2, at two different X-ray energies: 18 and 49 keV.

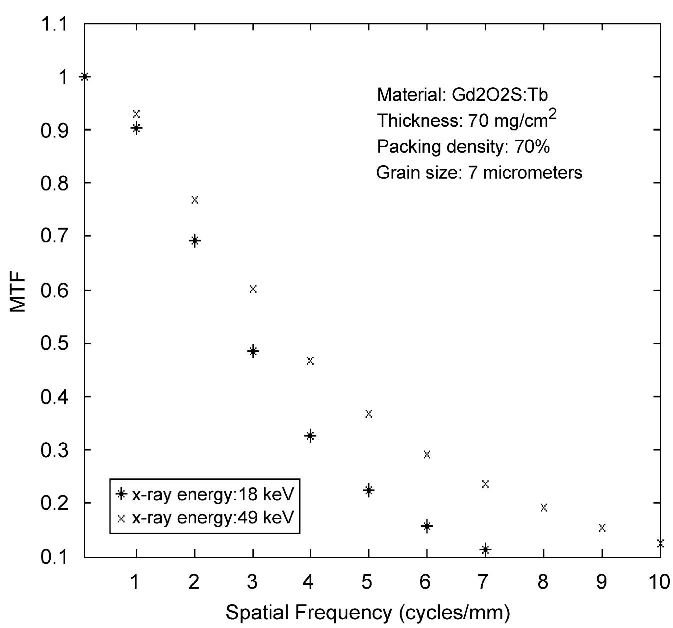

Fig. 2. The variation of MTF as a function of spatial frequency. MTF data are given for phosphor thickness 30 mg/cm^2, at two different X-ray energies: 18 and 49 keV.

According to the MTF results shown in Figs. 1 and 2, for higher X-ray energy photons, the phosphor screen was found to exhibit higher resolution properties in both cases. This is due to the following reason: light photons created by those X-ray photons, were generated within the phosphor screen closer to the mode of interest (transmission mode). Therefore, they give a narrower point spread function (PSF) curve because of the light spread in a restricted area. This sharper PSF, after Fourier transform contributes to a higher MTF curve. For example, for phosphor thickness equal to 70 mg/cm^2, the resolution (the frequency for which $\mathrm{MTF} = 0.1$) corresponds approximately to 7 lines/mm and 11 lines/mm at 18 and 49 keV, respectively.

A 70 mg/cm^2 screen exhibits better resolution properties at higher X-ray energies (e.g. 49 keV). Taking into account its high light output, under the same conditions, we come to the conclusion that the performance of a high packing density screen becomes better as phosphor thickness and X-ray energy increases. This property may be an advantage for radiographic applications.

4. Conclusion

It has been shown that high packing density X-ray powder screens provide in some cases better luminescent as well as resolution properties under similar conditions. In the present study, the performance of high packing density granular Gd_2O_2S:Tb was investigated for use in medical imaging diagnostic systems. It was found that high packing density screens appear their useful advantages for applications in X-ray radiology.

Acknowledgment

The project is co-funded by the European Social Fund and National Resources-EPEAEK II-ARXIMIDIS.

References

[1] G.F. Knoll, Radiation Detection and Measurement, second ed., Wiley, New York, 1989.
[2] M.J. Yaffe, J.A. Rowlands, Phys. Med. Biol. 42 (1997) 139.
[3] C.W.E. van Eijk, Phys. Med. Biol. 47 (2002) R85.
[4] S.M. Gruner, M.W. Tate, E.F. Eikenberry, Rev. Sci. Instrum. 73 (2002) 2816.
[5] G. Blasse, B.C. Grabmaier, Luminescent Materials, Spinger, Berlin, 1994.
[6] V.V. Nagarkar, S.R. Miler, S.V. Tipnis, A. Lempicki, C. Brecher, H. Lingertat, Nucl. Instr. and Meth. B. 213 (2004) 250.
[7] P. Liaparinos, I. Kandarakis, D. Cavouras, H. Delis, G. Panayiotakis, Med. Phys. 33 (2006) 4502.
[8] H.C. Van de Hust, Light Scattering by Small Particles, Wiley, New York, 1957.
[9] R. Morlotti, J. Photogr. Sci. 23 (1975) 181.
[10] H. Du, Appl. Optics. 43 (2004) 1951.
[11] J. Sempau, E. Acosta, J. Baro, J.M. Fernandez-Varea, F. Salvat, Nucl. Instr. and Meth. B. 132 (1997) 377.
[12] D. Brusa, G. Stutz, J.A. Riveros, J.M. Fernandez-Varea, F. Salvat, Nucl. Instr. and Meth. A. 379 (1996) 167.
[13] H.P. Chan, K. Doi, Phys. Med. Biol. 28 (1983) 109.
[14] J.H. Hubbell, P.N. Trehan, N. Singh, B. Chand, D. Mehta, M.L. Garg, R.R. Grag, S. Singh, S. Puri, J. Phys. Chem. Ref. Data. 23 (1994) 339.
[15] G. Peters, D.R. Wyman, M.S. Patterson, G.L. Frank, Phys. Med. Biol. 35 (1990) 1317.
[16] R. Graaff, M.H. Koelink, F.F.M. de Mul, W.G. Zijlstra, A.C.M. Dassel, J.G. Aarnoudse, Appl. Opt. 32 (1993) 426.